

FAILURE OF A COMBINE HARVESTER FRONT AXLE ANALIZA LOMA POLUOSOVINE KOMBajNA

Originalni naučni rad / Original scientific paper

UDK /UDC: 620.1:669.15`26`28

Rad primljen / Paper received: 05.06.2016

Adresa autora / Author's address:

¹) University of Novi Sad, Faculty of Technical Sciences,
Novi Sad, Serbia, email: sebab@uns.ac.rs

²) Purdue University, School of Engineering Technology,
West Lafayette, Indiana, USA

Keywords

- axle shaft
- decarburization
- fatigue crack initiation

Abstract

This paper describes the failure analysis expertise of the combine harvester axle shaft, made of heat treated Cr-Mo steel. The axle shaft was received as fractured after three years of operation. It was in a tempered- and case hardened condition. The failure zones were examined visually and with light- and scanning electron microscope. Also, chemical composition and Vickers hardness tests were carried out. The results indicated that fatigue is the dominant failure mechanism of the axle shaft. It was observed that the fatigue crack initiated at the tooth at four initiation regions with corresponding beach marks. The main cause that reduced the stress of crack initiation was decarburising in flanks of gear teeth. This was shown by the existence of ferrite in lathe martensite matrix in decarburized regions. Such finding is confirmed by a lower value of Vickers hardness in the flank region in relation to the sub-surface region, not affected by decarburisation.

INTRODUCTION

Shafts with circular cross section are invariably used for transmission of power, /1/. Axle shafts are generally used to connect wheel and differential for the purpose of power transmission and rotational motion. During operation, axle shafts are subjected to torsion and bending stresses due to self-weight or weights of components. Furthermore, possible misalignment between journal bearings may be one of the important factors in axle shaft stress /2, 3/. As a consequence, these rotating components are susceptible to fatigue by nature of their operation. Fatigue failures are generally of the torsion, torsion-bending and reversed bending type. However, to start the fatigue, a stress concentration in the dynamically stressed section must be present /4/. The stress concentrator may be of mechanical or metallurgical nature, or both. Additionally, in general, the stress concentrator may occur at the critical location, due to misalignment, defective lubrication or a metallurgical defect in form of non-metallic inclusions or some type of surface defect /5, 6/. In the present study, a failure analysis of the front axle shaft of combine harvester is shown. The

Ključne reči

- poluosovina
- razugljeničenje
- inicijacija zamorne prsline

Izvod

U ovom radu je opisana analiza loma poluosovine kombajna, koja je izrađena od termički obrađenog Cr-Mo čelika. Poluosovina je na analizu stigla prelomljena, nakon tri godine eksploatacije. Površinski sloj je kaljen i nisko-temperaturno otpuštan, dok unutrašnjost poluosovine odgovara poboljšanom stanju čelika. Ispitivanje na prelomljenoj površini je izvršeno vizuelno i uz pomoć svetlosnog i SEM mikroskopa. Takođe je izvršeno ispitivanje hemijskog sastava i tvrdoće prema Vickersu. Rezultati sugerišu da je do loma došlo usled zamora materijala, uzrokovano nastankom inicijalne prsline na boku zuba poluosovine, na četiri različita mesta sa jasnim linijama odmaranja. Glavni razlog nastanka zamornih prsline je razugljeničenje do kojeg je došlo na površini zuba. Ovo je potvrđeno postojanjem ferita u martenzitnoj osnovi u razugljeničenom području. Ovaj zaključak je dodatno potvrđen niskim vrednostima tvrdoće po Vickersu u razugljeničenoj oblasti u odnosu na sloj koji nije razugljeničen.

combine harvester was operational for three years or harvesting seasons. The combine harvester was used for grain and corn harvesting, that is, twice a year for approximately two months. The front axle shaft suddenly fractured during grain harvesting in 2012, without injuries to the operator. After a short examination, it was decided to perform an expertise to find the cause of failure.

EXPERIMENTAL PROCEDURE

The chemical composition of the failed axle shaft was determined by ARL-2460 spectrometer. Metallographic examinations are done with Leitz Orthoplan light microscope and JEOL JSM-6460LV scanning electron microscope (SEM), after standard metallographic preparation technique. Metallographic preparation consisted of grinding with a set of sandpapers (grit 100 to 2000), polishing with a diamond paste (6, 3, 1 and ¼ µm particle size) and etching with 3% nital (3% nitric acid solution in alcohol). The fracture surface was observed visually and by measuring device. Hardness is measured on the tooth top, flank and hardness profile is obtained from the gears bottom to the interior of the cross-section. Vickers hardness test with 5 kg

load is applied. Indentation distances are measured on a light microscope, by a specialized ocular lens (eyepiece) equipped with a scale. Hardness of axle shaft in various regions is measured by VEB HPS, a combined Brinell-Vickers measuring device. Hardness is measured on the tooth top, flank, and the hardness profile is obtained from the gears bottom to the interior of the cross-section.

RESULTS

Chemical analysis

Chemical composition of the 4140 steel according to AISI standard is shown in Table 1. It can be seen that the composition of the failed axle shaft material contains more Cr and S than the standard requirement.

Table 1. Chemical composition of failed axle shaft and AISI 4140 steel (wt.%).

Element	Failed axle shaft	AISI 4140 steel
%C	0.43	0.38-0.43
%Si	0.29	0.15-0.35
%Mn	0.823	0.75-1.00
%S	0.050	0.040
%Cr	1.392	0.80-1.10
%P	0.011	0.035
%Mo	0.245	0.15-0.25
%Cu	0.090	-
%Ni	0.069	-

Visual examination

The fractured surface is shown in Fig. 1. Fracture morphology reveals a torsion-bending fatigue as a result of crack development that started at four initiation regions, with multiple sites at specimen surface, with corresponding beach marks. The cracks initiated at tooth flank. Initiated cracks propagated and consecutively met, which is followed by the area of overload (final) fracture towards specimen centre. Visual examination reveals an adequate heat treatment with a relatively small overload section.

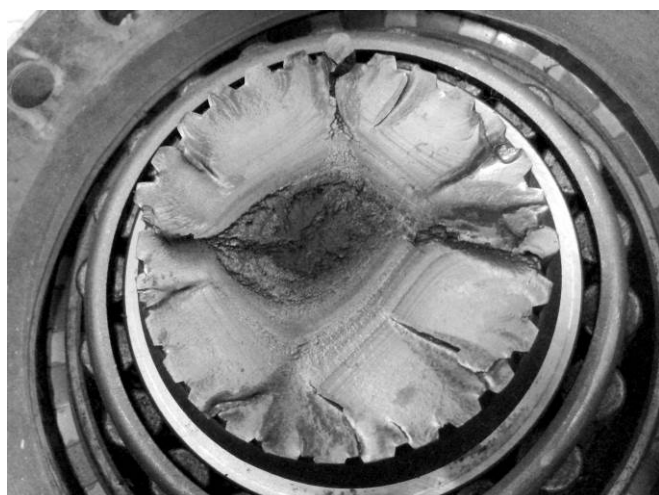


Figure 1. Macrograph of an axle shaft fractured surface with indicated fracture origins-initiation sites.

Macro- and microstructural testing

Macro testing is done at the surface and sub-surface regions of the specimen, Fig. 2. A macro image of the gear

tooth reveals that two regions are apparent: surface layer that appears to be case hardened (most probably induction hardened) and the inner section that probably corresponds to the microstructure obtained by tempering.

Sub-surface microstructure at 0.5 mm depth and inner section microstructure are shown in Fig. 3. In Figure 3a, a tempered martensite, typical for low temperature tempering heat treatment, is shown. In the inner section, a tempered martensite may be observed as well, however, the morphology is typical for through tempering process. This indicates that a through tempering process was conducted first, with a higher tempering temperature, thus increasing ductility. It was followed by case hardening and low temperature tempering to increase surface hardness and fatigue resistance by the prevention of crack initiation.

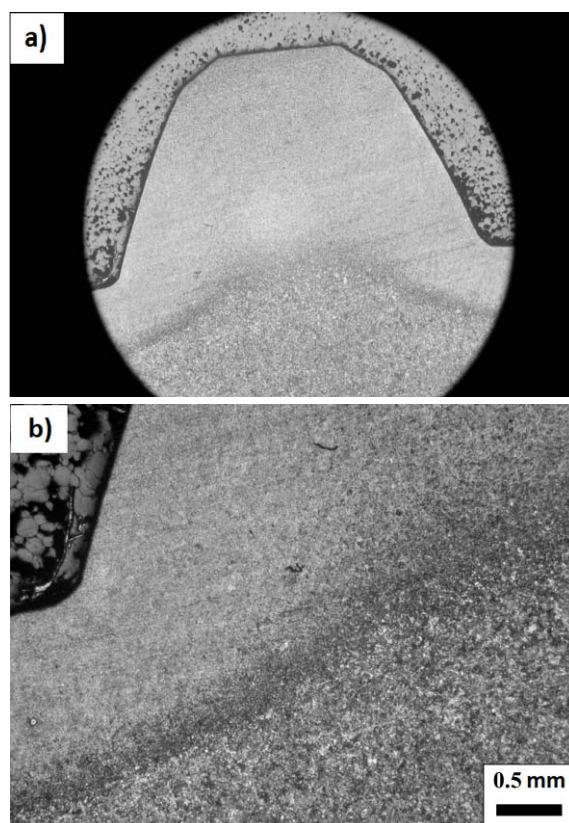


Figure 2. Sample microstructure: a) low magnification showing gear tooth geometry, b) intermediate layer microstructure.

In order to study the surface and sub-surface layer within the case hardened region, gears bottom land, tooth flank and top are examined, as to search for any signs of metallurgical defects, Figs. 4 and 5.

The microstructure of gears bottom land is shown in Fig. 4. Its morphology corresponds to case hardening and low temperature tempering. No differences between surface and sub-surface layers are visible.

Tooth surface (flank) microstructure is shown in Fig. 5. On the flank surface, a case hardening microstructure is visible. The surface layer is clearly brighter and with a different morphology than the sub-surface layer. Light microscopy- (LM) and SEM micrographs reveal the presence of ferrite isles in the tempered martensite matrix.

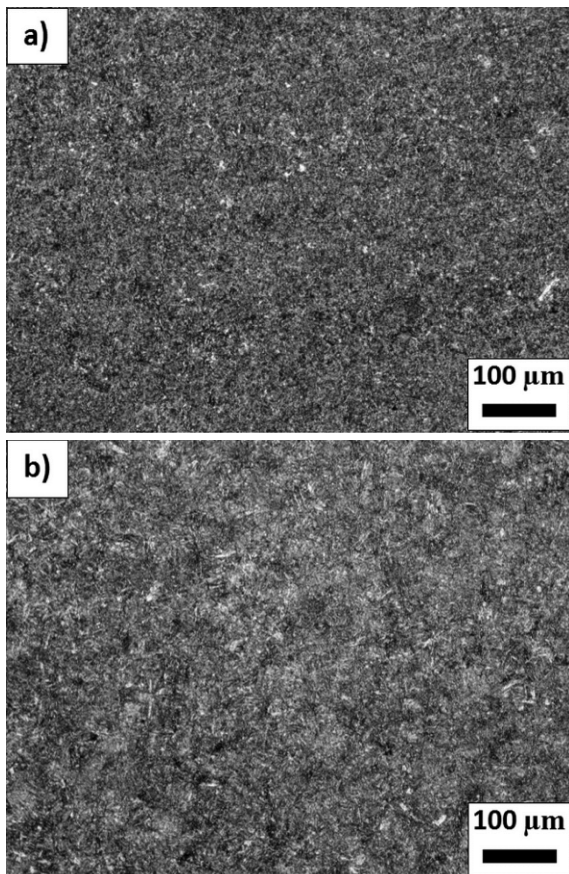


Figure 3. Failed axle shaft microstructure: a) surface; b) core.

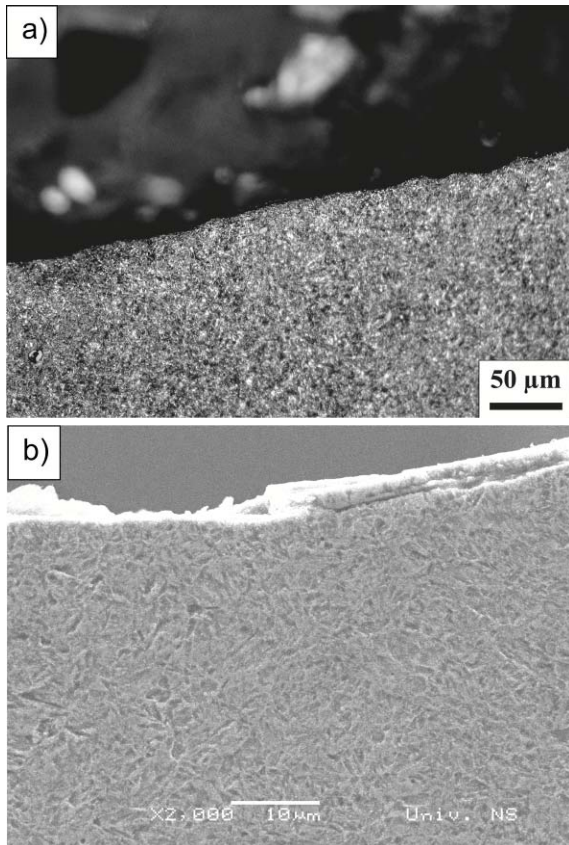


Figure 4. Gears bottom land: a) LM; b) SEM. No morphological differences between surface and sub-surface layer are observed.

Vickers hardness results

Vickers hardness results, measured on the tooth top, flank and from the gears bottom to the interior of the cross-section, are shown in Fig. 6. It can be seen that hardness of the tooth top and upper tooth flank are similar (471-473 HV5), followed by the mid- and lower section of the tooth flank (549 HV5), Fig. 6a. The highest hardness is obtained in the gears bottom (655 HV5), Fig. 8b. In Figure 8b, a hardness profile, measured from the gears bottom to the interior of the cross-section, up to the axle shaft centre is shown. It can be seen that in the surface layer, reaching 1 mm, a relatively high hardness is obtained, followed by a steep drop with nearly constant hardness values of 349-362 HV5, that reach up to the centre of the cross-section.

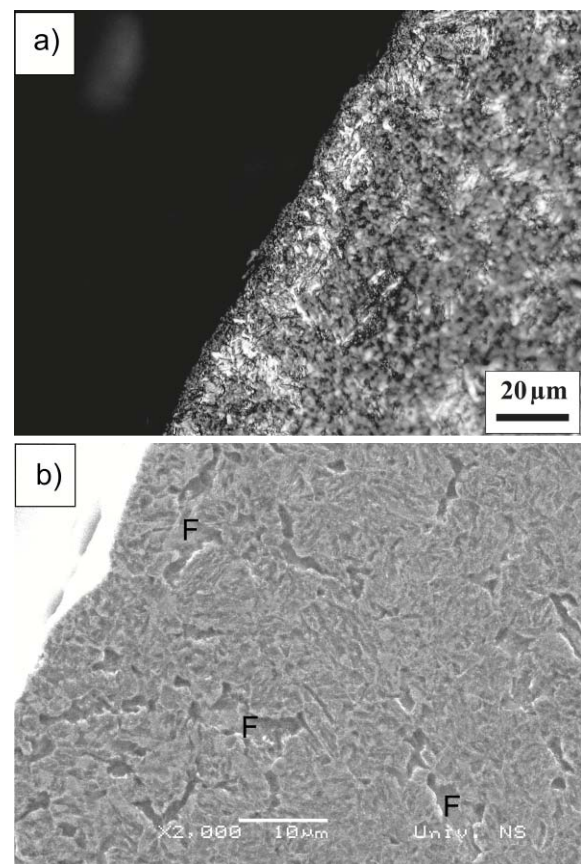


Figure 5. Tooth flank surface: a) LM; b) SEM. Ferrite isles may be observed in tempered martensite matrix.

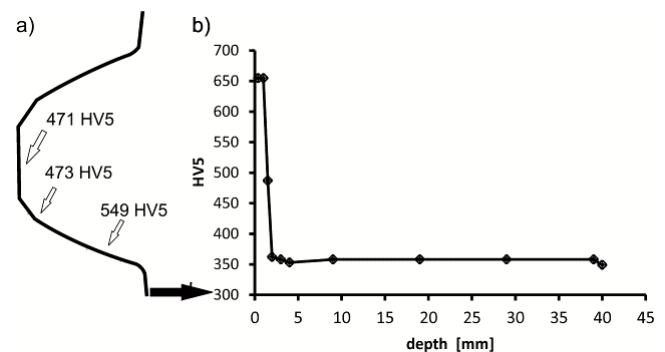


Figure 6. Hardness values at axle shaft cross-section: a) tooth top and flank; b) hardness profile at tooth bottom to the axle shaft centre.

DISCUSSION

Microstructure testing revealed the existence of two layers, a thin surface case hardened (probably induction hardened) and the inner tempered core. However, the microstructure of the surface layer varies with the tooth or gear section. The predominant tempered lathe martensite with ferrite isles is found in the tooth top and flank, while tempered lathe martensite is observed in the gears bottom land. This finding is supported by a decreased hardness in tooth top and flank regions where ferrite isles are observed. Ferrite isles may have appeared before heat treatment (quenching and tempering), most probably as the result of decarburisation. Furthermore, the decarburisation is more severe as the distance from the gears bottom land is greater. Obviously, based on microstructure and hardness measurements, the highest decarburisation occurred in external or exposed gear sections, such as the tooth. It is possible that the extent of the decarburization on the tooth flank is higher than evaluated in this expertize, since the surface might be worn out during operation. A decreased hardness on some tooth sections influenced the decrease in the stress required for fatigue crack initiation. However, the main reason for crack initiation is the presence of ferrite in the microstructure. This means the crack might initiate at the ferrite isle, even in a lower decarburized region if this region is more severely loaded as the tooth lower flank.

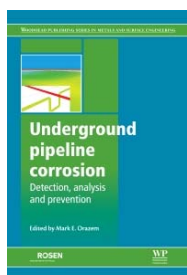
CONCLUSIONS

The obtained results indicate that the fracture was caused by fatigue, that started at the initiation site at the tooth flank or top. Microstructural and lower hardness results indicate that the surface was decarburised or partially decarburized before case hardening. After the case hardening process, a lower amount of carbon in the surface and sub-surface layers affected the hardness and therefore influenced a decreased stress required for fatigue crack initiation. The definite reason for premature fracture is found to be a defective heat treatment of the axle shaft.

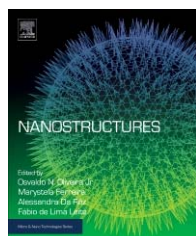
REFERENCES

1. Nanaware, G.K., Pable M.J. (2003), *Failures of rear axle shafts of 575 DI tractors*. Eng. Fail. Anal. 10 : 719-24.
2. Asi, O. (2006), *Fatigue failure of a rear axle shaft of an automobile*, Eng. Fail. Anal. 13: 1293-1302.
3. van Zyl, G., Al-Sahli, A. (2013), *Fail analysis of conveyor pulley shaft*, Case Stud. in Eng. Fail. Anal. 1 : 2213-2902.
4. Smallman, R., Bishop R., *Modern Physical Metallurgy & Materials Engineering*, Butterworth Heinemann, London, UK, 1999.
5. Sidjanin, L., *Engineering materials II*, University of Novi Sad, Faculty of Technical Sciences, Novi Sad, 1996.
6. Farrahi, G.H., Hemmati, F., Gangaraj, S.M., Samakhei, M. (2011), *Failure analysis of a four-cylinder diesel engine crankshaft made from nodular cast iron*, J Engine Res. 22 : 21-28.

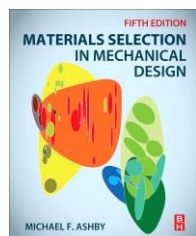
ELSEVIER STORE Wiley Online Library



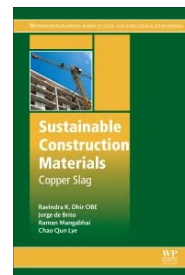
Underground Pipeline Corrosion, 1st Edition
Editor M. Orazem
Woodhead Publishing, Jan 2014
ISBN: 9780857095091
EISBN: 9780857099266



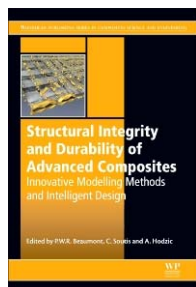
Nanostructures, 1st Edition
Eds: O. de Oliveira Jr.,
M. Ferreira, A. Luzia Da Róz,
F. Leite
Elsevier, Nov 2016
ISBN: 9780323497824



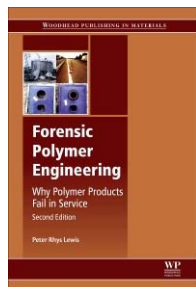
Materials Selection in Mechanical Design, 5th Edition
Michael F. Ashby
Butterworth-Heinemann, Nov 2016
ISBN: 9780081005996



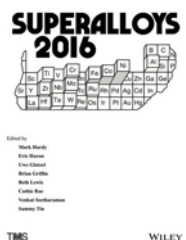
Sustainable Construction Materials, 1st Edition, Copper Slag
R.K. Dhir OBE, J. de Brito, R. Mangabhai,
C.Q. Lye
Woodhead Publishing, Oct 2016
ISBN: 9780081009864



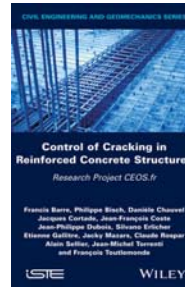
Structural Integrity and Durability of Advanced Composites, 1st Ed.
Innovative Modelling Methods and Intelligent Design
Eds. P. Beaumont, C. Soutis, A. Hodzic
Woodhead Publishing, May 2015
ISBN: 9780081001370
EISBN: 9780081001387



Forensic Polymer Engineering, 2nd Ed., Why Polymer Products Fail in Service
Peter R. Lewis
Woodhead Publishing,
June 2016
EISBN: 9780081007280



Superalloys 2016: Proceedings of the 13th International Symposium on Superalloys
Eds. M.C. Hardy, E.S. Huron, U. Glatzel, B. Griffin, B. Lewis, C. Rae, V. Seetharaman, S. Tin
Wiley, Nov. 2016
ISBN: 978-1-118-99666-9



Control of Cracking in Reinforced Concrete Structures: Research Project CEOS-9
F. Barre, P. Bisch, D. Chauvel, J. Cortade, J.-F. Coste, J.-P. Dubois, S. Erlicher, E. Gallitree, P. Labbé, J. Mazars, C. Rospars, A. Sellier, J.-M. Torrenti, F. Toutlemonde
Wiley, Sep. 2016
ISBN: 9781786300522
On-line ISBN: 97811119347088